Electronic Supplementary Information

The Effect of Pore Size and Layer Numbers of Metal-Porphyrin Coordination Nanosheets on Sensing DNA

Chenxi Liu,[a] Tianyu Wang,[a] Jing Ji,[b] Chiming Wang,[a] Hailong Wang,*[a] Peng Jin,[b] Wei Zhou,*[c] and Jianzhuang Jiang*[a]

[a] Beijing Key Laboratory for Science and Application of Functional Molecular and Crystalline Materials, Department of Chemistry, University of Science and Technology Beijing, Beijing 100083, China.
E-mail: hlwang@ustb.edu.cn (H.W.); jianzhuang@ustb.edu.cn (J.J.)
[b] School of Materials Science and Engineering, Hebei University of Technology, Tianjin 300130, China.
[c] NIST Center for Neutron Research, National Institute of Standards and Technology, Gaithersburg, Maryland 20899-6102, United States.
E-mail: wzhou@nist.gov (W.Z.)

Table of Content

Experimental section.

General remarks: Organic solvents and reagents from commercial sources were used directly without further treatment. 4-Hydroxymethylbenzaldehyde, 4′-(4-hydroxymethylphenyl)-2,2′:6′,2′′-terpyridine and 4′-(4-formylphenyl)-2,2′:6′,2′′-terpyridine were prepared according to the published procedures.[S1,S2,S3] 4'-([2,2':6',2''-Terpyridin]-4'-yl)-[1,1'-biphenyl]-4-carbaldehyde was prepared referring to the published procedure.[S2]

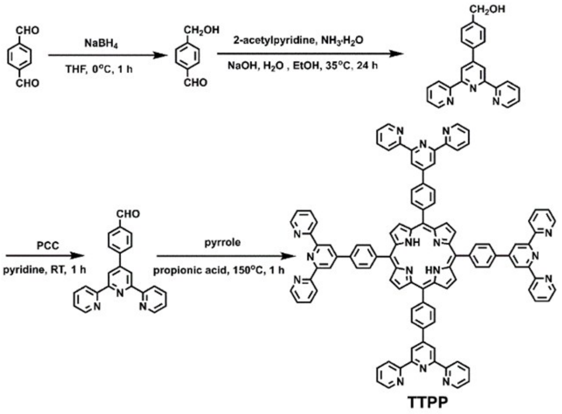

Scheme S1. Schematic synthesis and molecular structure of 5,10,15,20-tetrakis[4'-(terpyridinyl)phenyl]porphyrin (TTPP) (PCC = pyridinium chlorochromate).

Synthesis of 4′-(4-hydroxymethylphenyl)-2,2′:6′,2′′-terpyridine: To a solution of 4-hydroxymethylbenzaldehyde (1.36 g 10.0 mmol) in ethanol (50 mL), 2-acetylpyridine (2.42 g, 20.0 mmol), sodium hydroxide (0.60 g, 20.0 mmol), and aqueous ammonia (30 mL, 28%) were added. The resultant mixture was stirred at 35 °C for 24 h. After cooling down, the crude product was obtained by filtration and washing with ethanol (3 × 10 mL). The white product was obtained by recrystallization from ethanol with the yield of 25% (0.84 g). ^{1}H NMR (400 MHz, DMSO-d_6, δ): 9.61 (s, 4H), 9.55 (d, J = 4.0 Hz, 2H), 8.77 (m, 4H,), 8.38 (d, *J* = 8.0 Hz, 2H), 8.24 (m, *J* = 5.8 Hz, 1.2 Hz, 2H), 5.67 (d, *J* = 5.6 Hz, 2H), 3.00 (t, *J* = 6.0 Hz, 1H).

Synthesis of 4′-(4-formylphenyl)-2,2′:6′,2″-terpyridine: To a solution of 4′-(4-hydroxymethylphenyl)-2,2′:6′,2″-terpyridine (2.0 g, 5.9 mmol) in pyridine (100 mL), pyridinium chlorochromate (PCC, 2.6 g, 12.0 mmol) was added. The mixture was stirred at room temperature for an hour and the solvent was evaporated in vacuum. The crude product was purified by column chromatography on silica gel (CH_2Cl_2:MeOH = 97:3 (*v*:*v*)) to afford product as white solid with a yield of 70% (1.4 g). ^{1}H NMR (400 MHz, $CDCl_3$, δ): 10.11 (s, 1H), 8.77 (s, 2H), 8.74 (d, *J* = 3.6 Hz, 2H), 8.69 (d, *J* = 7.6 Hz, 2H), 8.05 (m, *J* = 11.2 Hz, 6.4 Hz, 4H), 7.90 (m, 2H), 7.38 (m, 2H).

Synthesis of 5,10,15,20-tetrakis[4'-(terpyridinyl)phenyl]porphyrin (TTPP): To a refluxing propionic acid (50 mL) solution of 4′-(4-formylphenyl)-2,2′:6′,2″-terpyridine (1.7 g, 5.0 mmol), a solution of pyrrole 0.34 mL (5.0 mmol) in propionic acid (1 mL) was added dropwisely. The resulting mixture was stirred and heated at 150 °C for an hour. After being cooled to ambient temperature, the mixture was added into water (200 mL) and kept at 0 °C overnight. The purple precipitate was obtained by filtration and washed with MeOH (3 × 50 mL) and $CHCl_3$ (3 × 20 mL) in a total yield of 25%. ^{1}H NMR (400 MHz, $CDCl_3$, δ): 9.09 (s, 8H), 8.99 (s, 8H), 8.80 (d, *J* = 4.0 Hz, 8H), 8.78 (d, *J* = 8.0 Hz, 8H), 8.42 (d, *J* = 8.0 Hz, 8H). 8.33 (d, *J* = 8.0 Hz, 8H), 7.94 (m, *J* = 8.0 Hz, 8H), 7.40 (m, *J* = 5.6 Hz, 8H), –2.65(s, 2H); UV–vis ($CHCl_3$): λ_{max} (log ε) = 424 (6.23), 519

(4.92), 554 (4.77), 593 (4.53), 650 nm (4.56); MS (MALDI-TOF) *m/z*: $[M + H]^+$ calcd for $C_{104}H_{66}N_{16}$, 1539.6; found, 1539.6. Anal. calcd for $C_{104}H_{66}N_{16}$ $CHCl_3$: C 76.01, H 4.07, N 13.51; found: C 76.08, H 3.90, N 13.22.

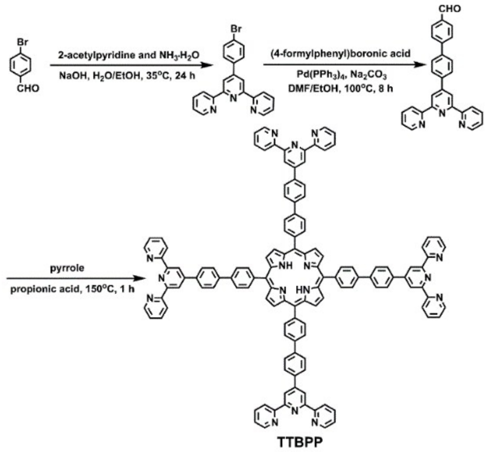

Scheme S2. Schematic synthesis and molecular structure of 5,10,15,20-tetrakis[4'-(terpyridinyl)-1,1'-biphenyl]porphyrin (TTBPP).

Synthesis of 5,10,15,20-tetrakis[4'-(terpyridinyl)-1,1'-biphenyl]porphyrin (TTBPP) and preparation of Co-TTBPP nanosheet: To a refluxing propionic acid (50 mL) solution of 4'-([2,2':6',2''-terpyridin]-4'-yl)-[1,1'-biphenyl]-4-carbaldehyde (1.65 g, 4.0 mmol), a solution of pyrrole (0.28 mL 4.0 mmol) in propionic acid (1 mL) was added drop-wise. The resulting mixture was stirred and heated at 150 °C for an hour. After being cooled to ambient temperature, the mixture was added into water (100 mL) and kept at 0 °C overnight. The purple precipitate was obtained by filtration and washing by MeOH (3 × 50 mL) and $CHCl_3$ (3 × 20 mL) with a yield of 34% (0.62 g). ^1H NMR (400 MHz, $CDCl_3$, δ): 9.02 (s, 8H), 8.90 (s, 8H), 8.80 (d, *J* = 4.0 Hz, 8H), 8.74 (d, *J* = 8.0 Hz, 8H), 8.39 (d, *J* = 8.0 Hz, 8H), 8.19 (d, *J* = 8.0 Hz, 8H), 8.12 (d, *J* = 8.0 Hz, 16H), 7.94 (m, 8H), 7.41 (t, *J* = 8.0 Hz, 8H), –2.62 (s, 2H); UV–vis ($CHCl_3$): λ_{max} (log ε) = 425 (4.47), 519 (3.06), 556 (2.94), 593 (2.62), 650 nm (2.66); MS (MALDI-TOF) *m/z*: $[M + H]^+$ calcd for $C_{104}H_{66}N_{16}$, 1843.7; found, 1843.9. Anal. calcd for $C_{128}H_{82}N_{16}$ $CHCl_3$: C 81.78, H 4.52, N 11.83; found: C 81.82, H 4.49, N 11.87. Preparation of Co-TTBPP nanosheet follows the same procedure of Co-TTPP nanosheet except using a chloroform solution of TTBPP (0.05 mg mL^{-1}, 2.7×10^{-5} M) instead of TTPP (0.1 mg mL^{-1}, 6.5×10^{-5} M).

Physical characterization: NMR spectra were collected on a Bruker DPX 400 spectrometer in $CDCl_3$ and DMSO-d_6 with the reference of residual solvent resonance (δ = 7.26 ppm for $CDCl_3$ and δ = 2.50 ppm for DMSO-d_6) relative to $SiMe_4$. Elemental analysis was performed on an Elementar Vavio El III elemental analyzer. Electronic absorption spectra were recorded on a Hitachi U-2910 spectrophotometer. MALDI-TOF mass spectra were determined on a Bruker BIFLEX III ultra-high-resolution mass spectrometer. Fluorescence analyses were carried out on a HITACHI F-4500 spectrometer. XPS spectra were conducted on an ESCALAB 250Xi system. Al Kα X-ray (6 mA × 12 KV) was utilized as the irradiation source, and all measurements were performed in the CAE mode for selective elements with the reference of C 1s (284.8 eV). Morphologies of nanosheets were checked using an atomic force microscope (Bruker Multimode 8 system) with a silicon cantilever in tapping mode. TEM images were collected at 100 kV with HITACHI HT7700 transmission electron microscopy. Energy dispersive spectroscopy (EDS) mapping images of nanosheets on Cu grids were collected by transmission electron microscopy (JEM-2100F) at an operation voltage of 200 kV. Powder X-ray diffraction (XRD) patterns were recorded with a Shimadzu XRD-

6000 powder X-ray diffractometer, using Cu Kα radiation (λ = 1.5406 Å). The Co-TTPP nanosheets fabricated by liquid-liquid interfacial method were acutely degassed for 24 hours at 100^{o}C using a Micromeritics ASAP 2020 plus surface area analyser, affording activated sample. The sequential gas sorption isotherms were determined employing the same instrument. The particular test temperatures, 77 and 196 K were handled in respective bathes of liquid nitrogen and a dry ice-acetone slurry.

Treatment of various substrates: Prior to atomic force microscopy (AFM) measurement, the protective film of mica sheet (1.0 cm × 1.0 cm) was torn off. Before UV–vis absorption measurement, the quartz substrate was washed with detergent for three times and soaked in a solution of H_2O_2/H_2SO_4 (v:v = 1: 1) for 24 hours, then rinsed with water and ethanol, respectively. After repetition of this series of operation for three times, the quartz sheets were sonicated for 5 minutes in Milli-Q water twice and then dried under a N_2 stream. Finally, the quartz substrate was hydrophobically functionalized using ferric stearate. It is worth noting that the quartz substrates utilized in DNA sensing experiment were treated in the same manner except without the treatment of ferric stearate. For X-ray photoelectron spectroscopy (XPS) measurement, Si (100) wafers (5.0 mm × 5.0 mm) were washed with detergent, and then sonicated in Milli-Q water and ethanol for 10 minutes, respectively. These treatments were performed for three times. The clean Si wafers were stored in ethanol for use. For photocurrent measurement, indium tin oxide (ITO) electrode (1.0 cm × 2.0 cm) was used, which was washed with detergent for three times and sonicated in Milli-Q water for 10 minutes, then rinsed with ethanol and sonicated in $CHCl_3$ for 10 minutes. These treatments were cycled for three times and dried to guarantee the resistance of clean ITO sheet less than 10 ohmsq^2 and the transmittance more than 83%.

Preparation of nanosheets: A chloroform solution of TTPP (0.1 mg mL^{-1}, 6.5×10^{-5} M) was used over all LB experiments. A Nima 516 trough (500 cm^2) was repeatedly cleaned using absorbent cotton soaked in ethanol and chloroform, respectively, which was then filled with an aqueous solution of MCl_2 (M = Co^{2+}, Ni^{2+}, and Fe^{2+}, 1 mM) as subphase. Under a paper Wilhelmy plate (1.0 cm × 1.7 cm), surface pressure-molecular area (π-a) isotherm measurement was conducted on a Nima system by driving two barriers at a pressing speed of 35 mm min^{-1}. To fabricate uniform and monolayer nanosheet (Co-TTPP, Ni-TTPP, and Fe-TTPP) on a subphase, a chloroform solution of TTPP with an optimized volume of 150 μL was dropwisely spread onto the corresponding subphase. After the reaction proceeding for 15 minutes at 25 °C, metal-organic coordination monolayer was generated on the air-water interface. By horizontally dipping, these monolayers were sequentially accumulated to different substrates to precisely control the layer number of the substrate-supported nanosheets. Before next transfer of monolayer, the nanosheets on different substrates were bathed in water for 10 minutes to exclude uncoordinated metal ions, then immersed in $CHCl_3$ for 10 minutes to eliminate the unreacted TTPP ligand. The obtained nanosheet was dried under a N_2 stream. Such treatment cycle was repeated for twice. As a reference, TTPP nanosheet was also prepared following the same procedure of Co-TTPP nanosheet except using pure water to replace metal ion subphase. At the end of this section, it is worth noting that, in order to probe the porosity information of Co-TTPP nanosheets, liquid-liquid interfacial method was used to prepare bulk material due to the difficulty in accumulating enough sample by the LB method. The well matched peak at 7.2° in their powder X-ray diffraction pattern confirms the same structure, Fig. S5. As a consequence, the obtained porosity information of Co-TTPP nanosheets prepared by liquid-liquid interfacial method should be agreement with that of sample fabricated by the LB method, Fig. S23. For the liquid-liquid interfacial method, a $CoCl_2$ (10 mM) aqueous solution (40.0 mL) of was slowly added on a chloroform solution (40.0 mL) of TTPP (6.5×10^{-4} M) in a 100 mL beaker. After a week, Co-TTPP nanosheets were obtained.

Photocurrent measurement: Photoelectric conversion was measured on the CHI 760E workstation. A three-electrode cell was assembled by ITO electrode modified by five-layer Co-TTPP nanosheet as working electrode (Co-TTPP/ITO electrode), a platinum wire as counter electrode, and an Ag^+/Ag electrode as reference electrode. The working electrode was fixed at 0 V versus Ag^+/Ag electrode.[S4] The cell was filled with an acetonitrile solution of tetra-*n*-butylammonium hexafluorophosphate (0.1 M) and triethanolamine (TEOA, 0.1 M) as sacrificial donor reagent. After purging N_2 stream for 20 minutes, a xenon lamp equipped with a 395 nm cut-off filter was used to illuminate Co-TTPP/ITO electrode. Furthermore, the Co-TTPP/ITO electrode was immersed in a 1,2-dichlorobenzene solution of fullerene (30 mM) for 12 hours, then washed with excessive 1,2-dichlorobenzene and acetonitrile, then dried under a nitrogen stream for photocurrent measurement. The amount of encapsulated C_{60} molecules in Co-TTPP nanosheets was determined as below: 1.32 mg C_{60}-doped Co-TTPP nanosheet scraped from substrate-supported film was dissolved in the aqueous solution of NaOH (0.5 M). The obtained aqueous solution was extracted with toluene. C_{60} was obtained by the purification of column chromatography on silica gel with toluene as eluent. The amount of C_{60} (0.03 mg per 1.30 mg Co-TTPP nanosheets) was deduced on the UV−vis analysis.

DNA detection: Both sides of a piece of quartz sheet (1.0 cm × 5.0 cm) were modified by Co-TTPP nanosheet with the same layer number for DNA sensing. Electronic absorption spectra were used to make sure the substrate-supported nanosheets with the same number of accumulated monolayers. Different nanosheets on quartz substrate were immersed in various solutions containing single-stranded DNA (ssDNA) and double-stranded DNA (dsDNA). After removal of nanosheets, the emission of solution was examined.

Computational details: All spin-polarized first-principles calculations were performed by using the Perdew-Burke-Ernzerhof (PBE)[S5] exchange–correlation functional as implemented in the Vienna ab initio simulation package (VASP).[S6,S7] A cutoff energy of 350 eV was set for the plane wave basis set. To avoid the interactions between slabs and their periodic images, a vacuum space of 15 Å was applied along the z-direction in the supercells. The k-points of 1×1×1 were generated using the Monkhorst-Pack method. The convergence thresholds for the energy and force are 10^{-4} eV and 0.05 eV $Å^{-1}$, respectively.

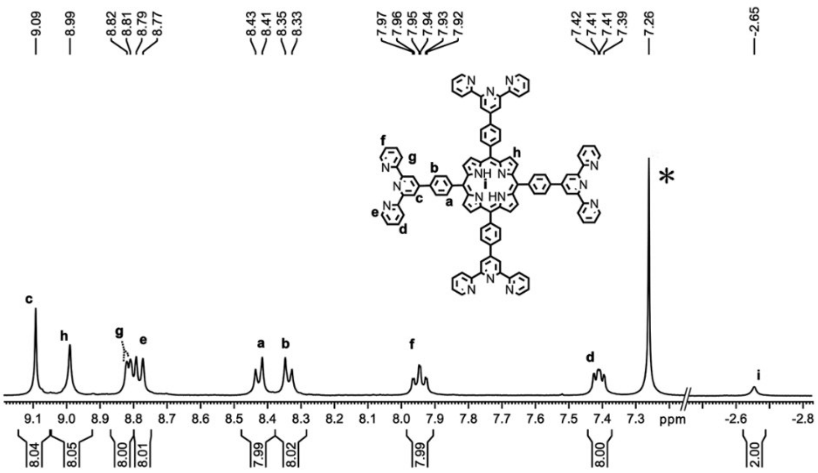

Fig. S1 ^{1}H NMR spectrum of TTPP in $CDCl_3$. * denotes the $CDCl_3$ solvent impurity.

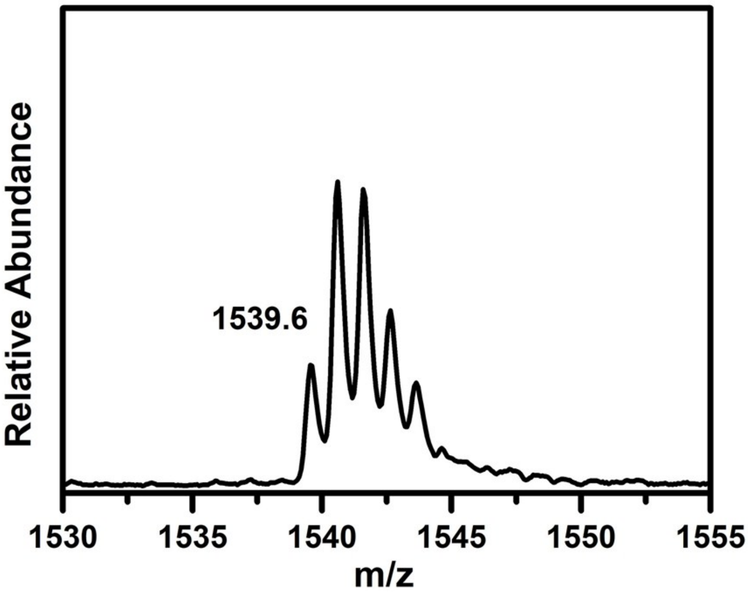

Fig. S2 Mass spectrum of TTPP.

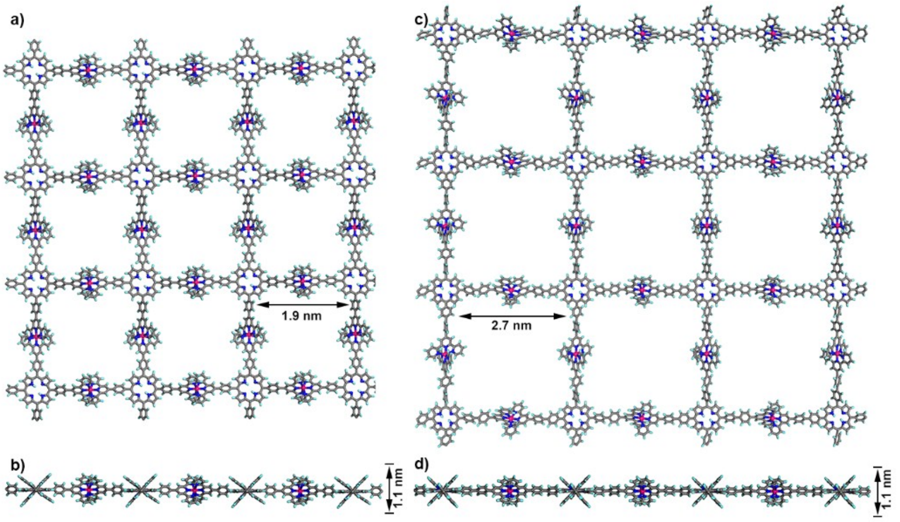

Fig. S3 Structures of Co-TTPP monolayer (in tope view (a) and side view (b) and Co-TTBPP monolayer in tope view (c) and side view (d) without including chloride ions (C: grey; N:blue; Co: pink; H: cyan).

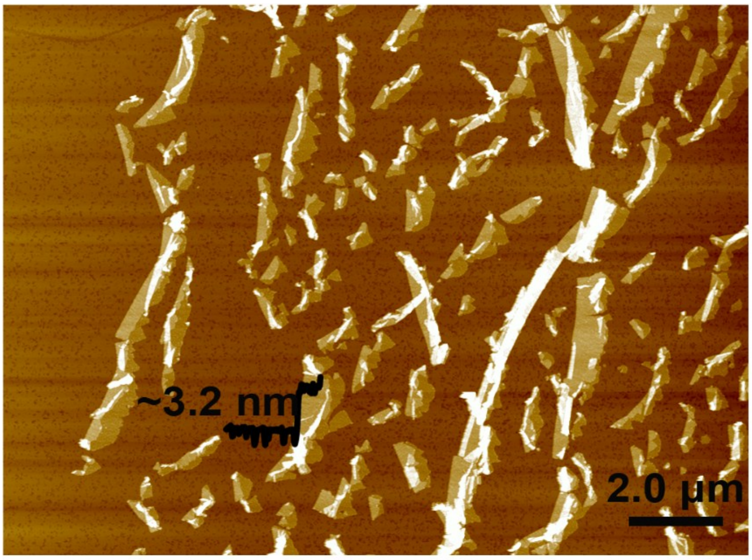

Fig. S4 AFM topographic image of TTPP nanosheet on mica substrate, showing the height of 3.2 nm between monolayer and mica substrate.

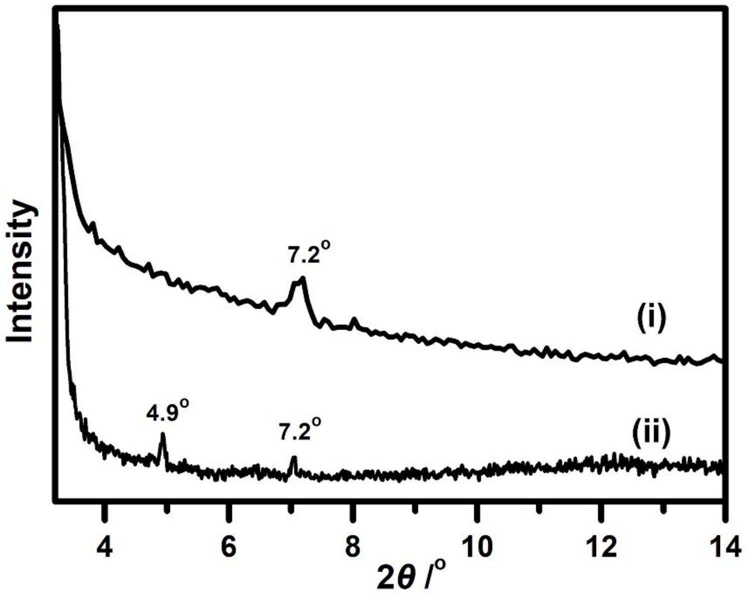

Fig. S5 Powder X-ray diffraction profiles of Co-TTPP nanosheets fabricated by LB (i) and liquid-liquid interfacial method (ii).

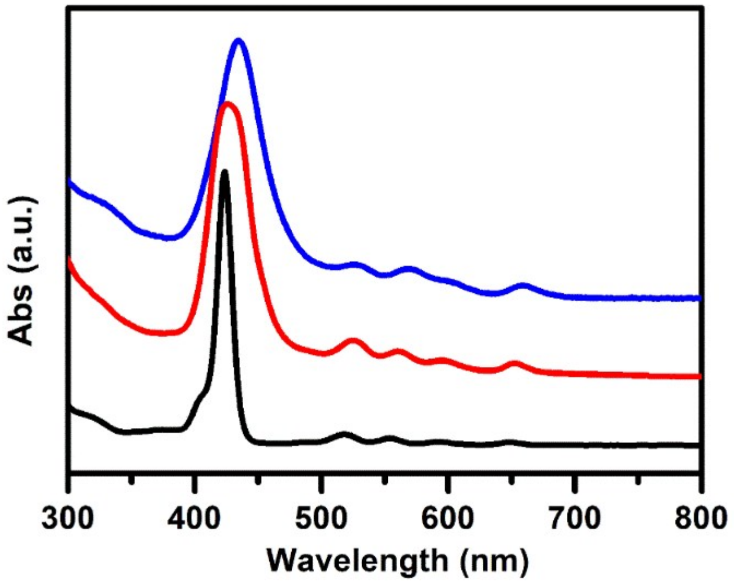

Fig. S6 Electronic absorption spectra of TTPP nanosheet (red line) and Co-TTPP nanosheet (blue line) on quartz substrate for a comparison with TTPP in $CHCl_3$ solution (black line).

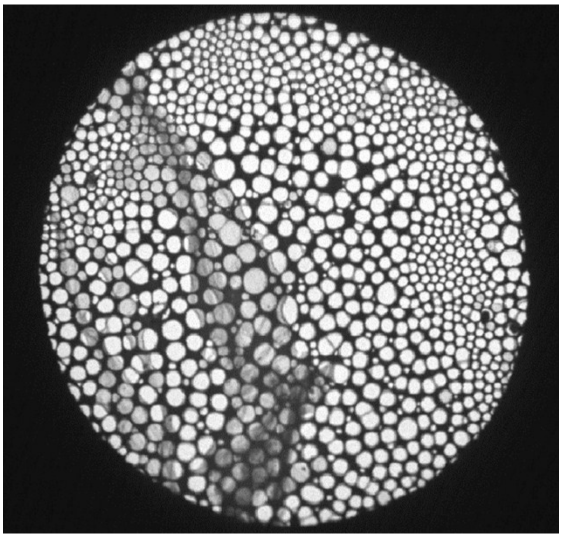

Fig. S7 TEM image of Co-TTPP nanosheet (the visual circle diameter *ca*. 115 μm).

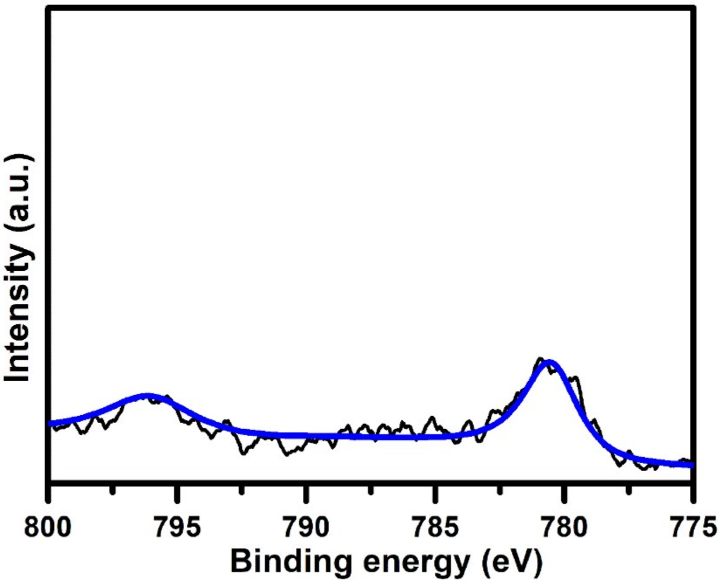

Fig. S8 High-resolution Co 2p photoemission spectrum of Co-TTPP nanosheet (black line: experimental; blue line: fitting).

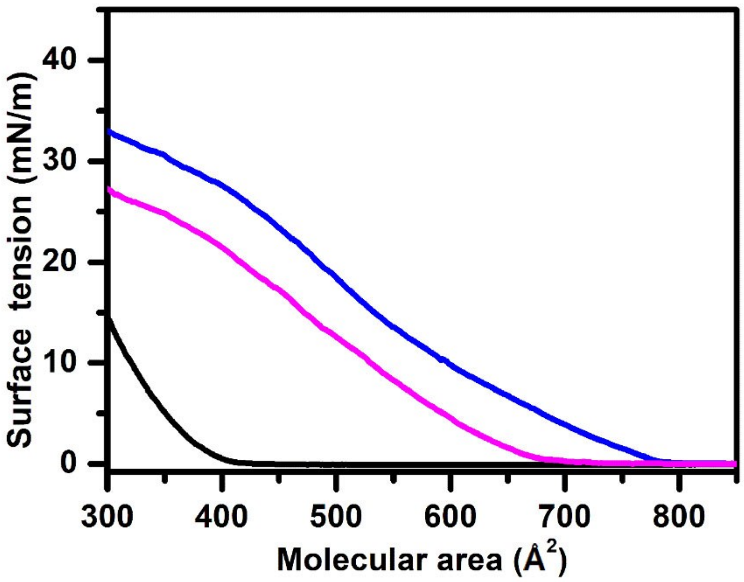

Fig. S9 Surface pressure-molecular area (π-a) isotherms for Ni-TTPP (pink line), Fe-TTPP (blue line) and TTPP (black line) nanosheets.

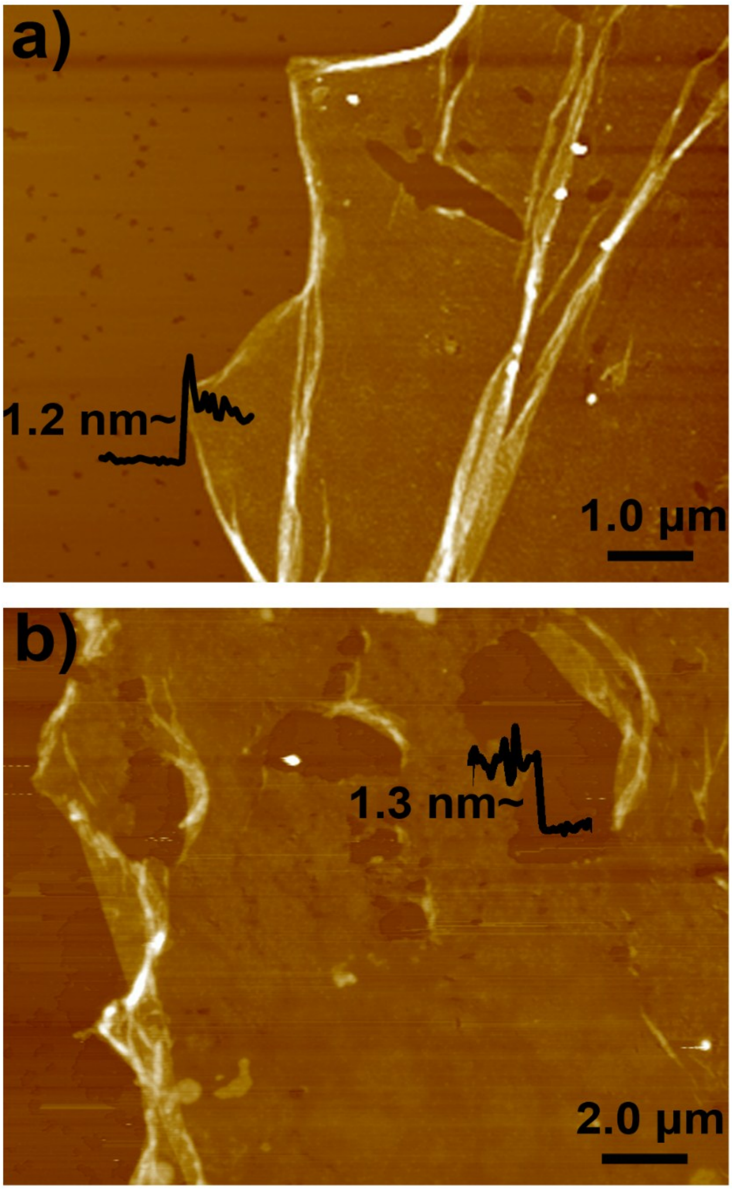

Fig. S10 Tapping-mode AFM images with height profile measured along the black line of Ni-TTPP (a) and Fe-TTPP (b) monolayers.

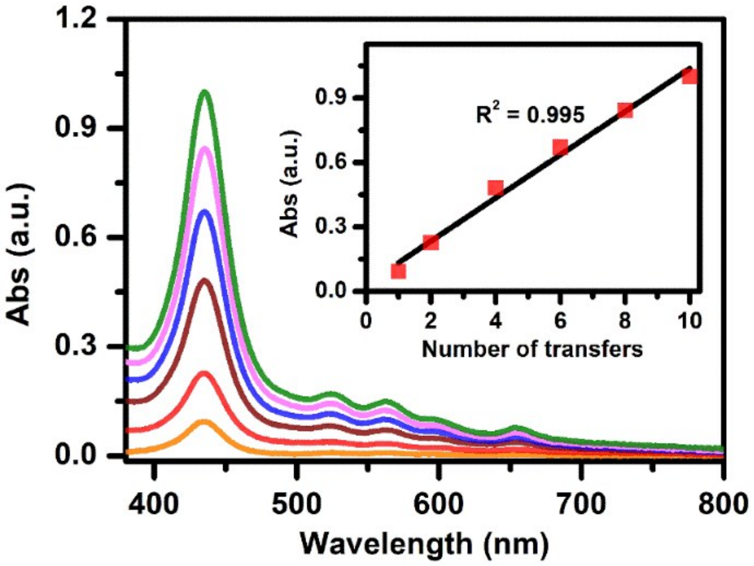

Fig. S11 Electronic absorption spectra of Ni-TTPP nanosheets with different layer number on quartz. The inset shows a linear relationship between the maximum absorbance of Soret band at 435 nm and layer number.

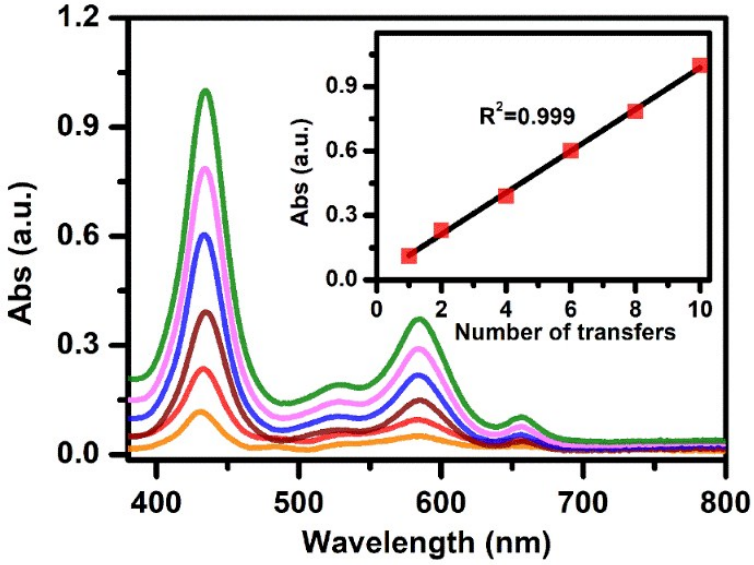

Fig. S12 Electronic absorption spectra of Fe-TTPP nanosheets with different layer number on quartz. The inset shows a linear relationship between the maximum absorbance of Soret band at 435 nm and layer number.

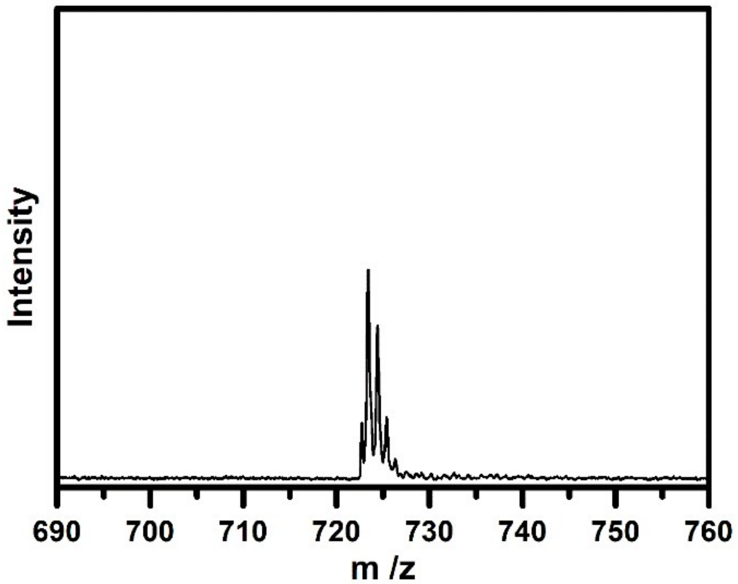

Fig. S13 MALDI-TOF spectrum of fullerene released from decomposed Co-TTPP nanosheet.

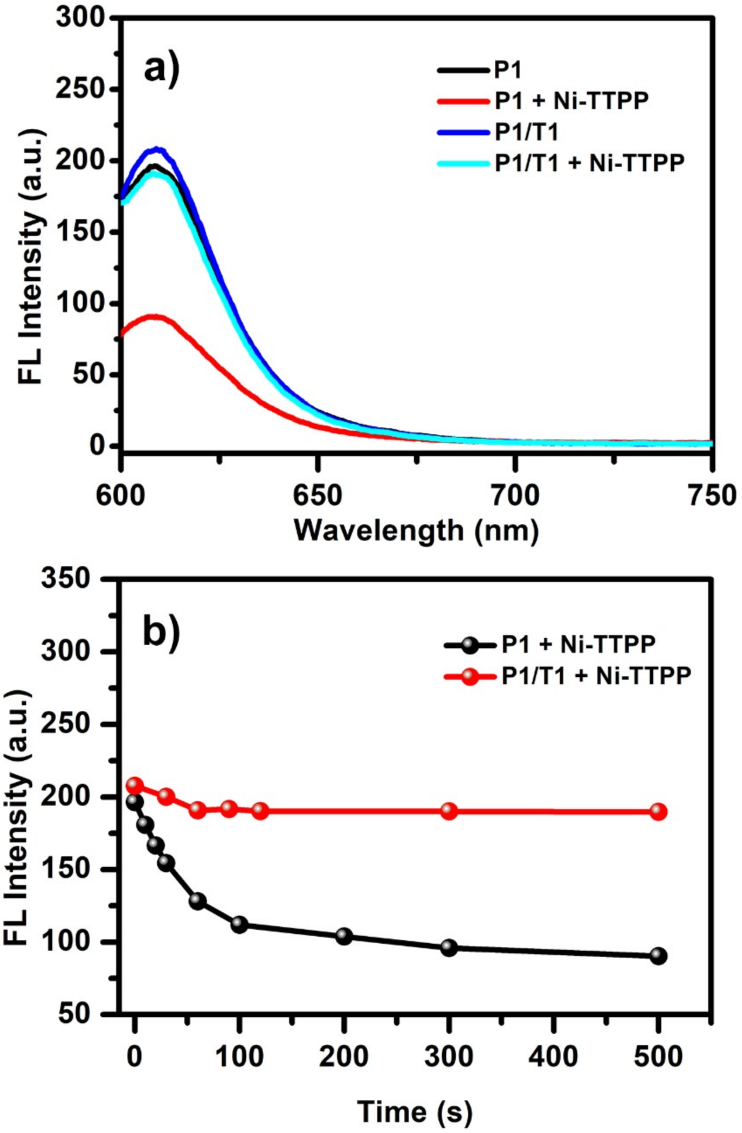

Fig. S14 (a) Fluorescence spectra of Texas red-labeled ssDNA (P1) with the excitation wavelength of 585 nm at different experimental conditions: P1, P1 + T1, P1 + Ni-TTPP, and P1/T1 + Ni-TTPP (the concentrations of P1 and T1 are 1 nM and 10 nM, respectively); (b) time-dependent emission intensity at 611 nm of P1 and P1/T1 in the existence of Ni-TTPP nanosheet on quartz substrate.

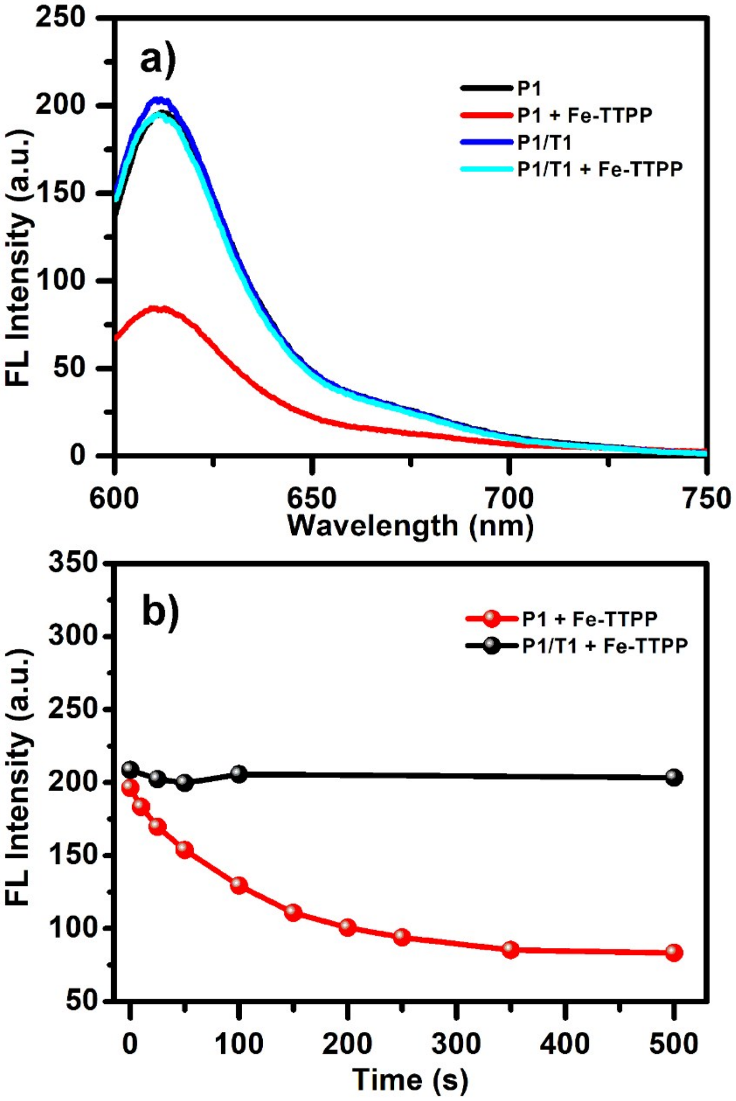

Fig. S15 (a) Fluorescence spectra of Texas red-labeled ssDNA (P1) with the excitation wavelength of 585 nm at different experimental conditions: P1, P1 + T1, P1 + Fe-TTPP, and P1/T1 + Fe-TTPP (the concentrations of P1 and T1 are 1 nM and 10 nM, respectively); (b) time-dependent emission intensity at 611 nm of P1 and P1/T1 in the existence of Fe-TTPP nanosheet on quartz substrate.

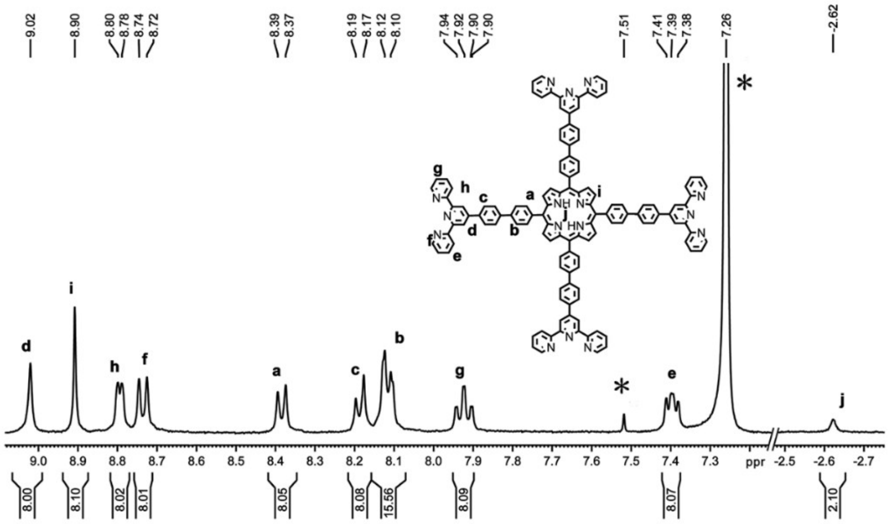

Fig. S16 ^{1}H NMR spectrum of TTBPP in $CDCl_3$. * denotes the $CDCl_3$ solvent impurity.

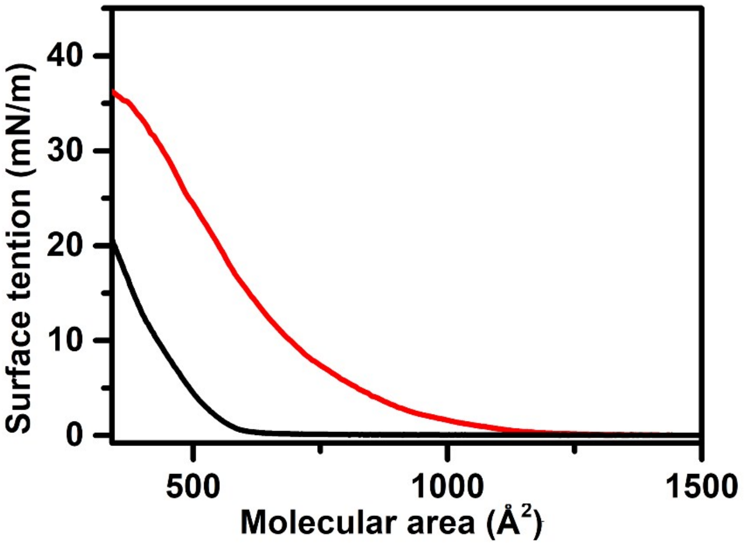

Fig. S17 Surface pressure-molecular area (π-a) isotherms for Co-TTBPP (red) and TTBPP (black) nanosheets.

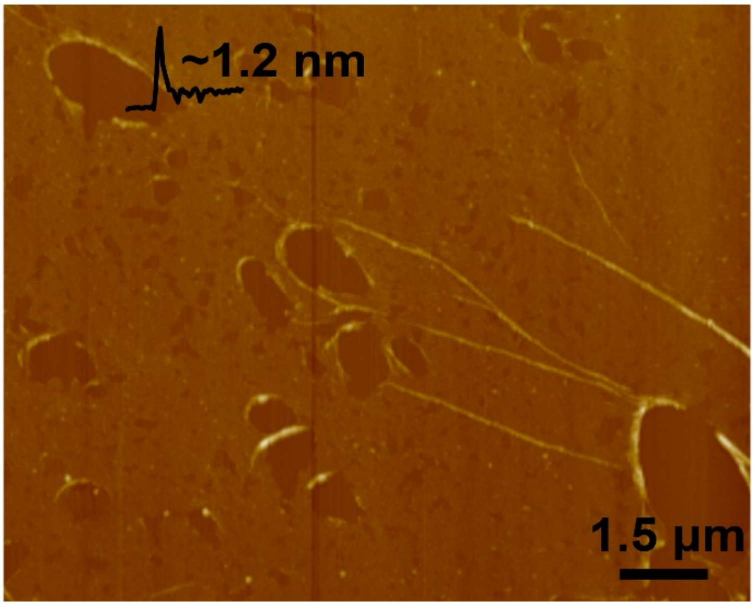

Fig. S18 Tapping-mode AFM image with height profile measured along the black line of Co-TTBPP monolayer.

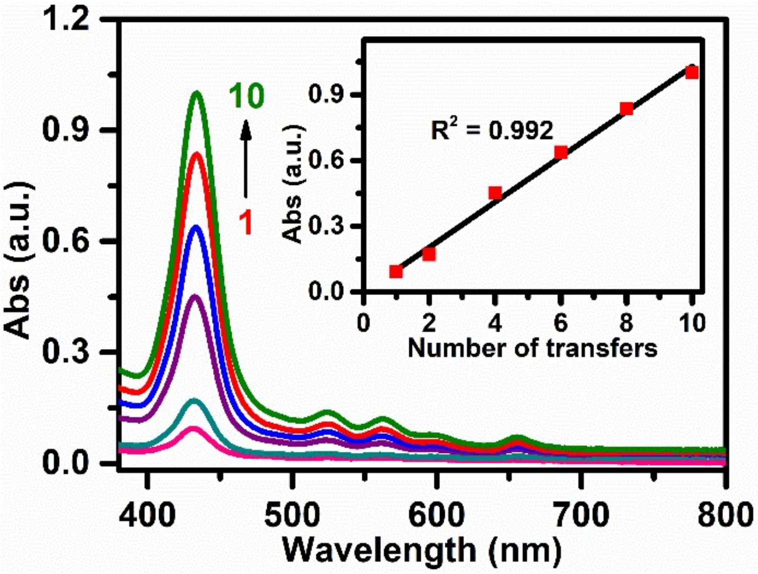

Fig. S19 Electronic absorption spectra of Co-TTBPP nanosheets with different layer number on quartz. The inset shows a linear relationship between the maximum absorbance of Soret band at 434 nm and layer number.

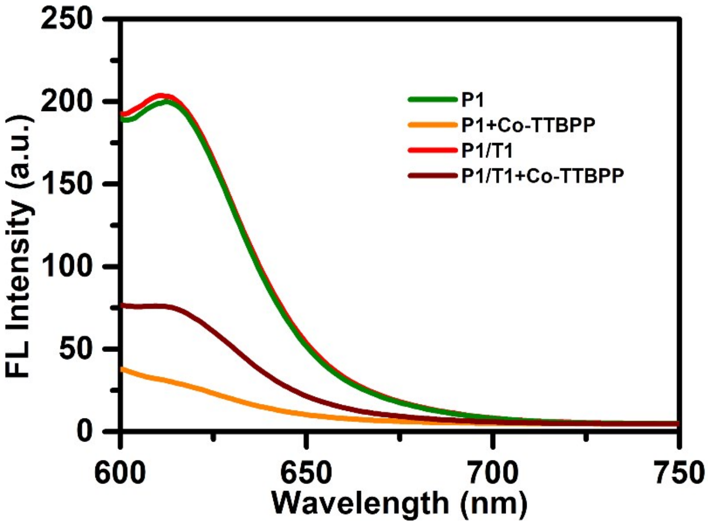

Fig. S20 Fluorescence spectra of Texas red-labeled ssDNA (P1) with the excitation wavelength of 585 nm at different experimental conditions: P1, P1 + T1, P1 + Co-TTBPP, and P1/T1 + Co-TTBPP (the concentrations of P1 and T1 are 1 nM and 10 nM, respectively).

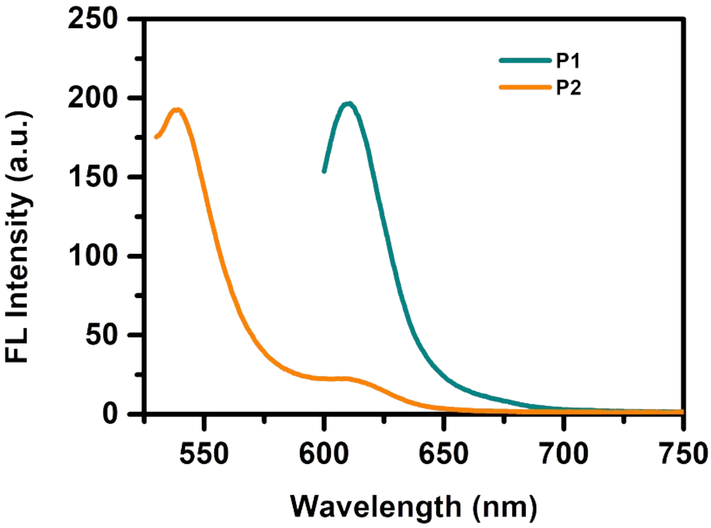

Fig. S21 Fluorescence spectra of DNA probes P1 and P2 with the excitation wavelengths of 585 nm and 490 nm, respectively.

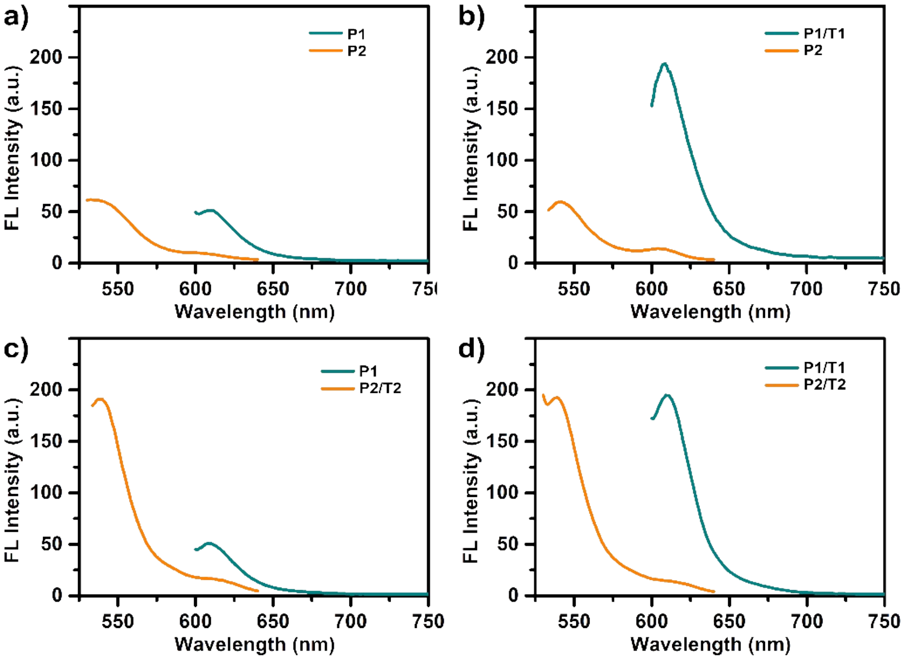

Fig. S22 Fluorescence spectra for multiplexed detection using ten-layer Co-TTPP nanosheets: probe mixture (P1 + P2) showing (a) in the absence of T1 and T2; (b) in the presence of T1 but absence of T2; (c) in the presence of T2 but absence of T1; (d) in the presence of both T1 and T2. Fluorescence signals of P1 and P2 were collected with the excitation wavelengths of 585 nm and 490 nm, respectively, and the concentrations of P1, P2, T1, and T2 are 1.0, 1.0, 10.0, and 10.0 nM, respectively.

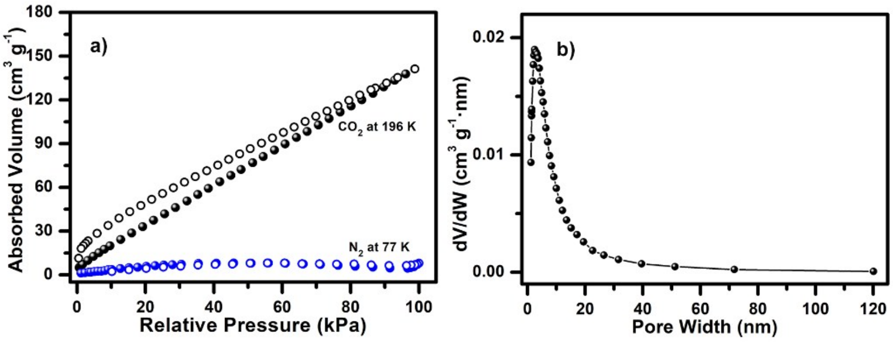

Fig. S23 (a) N_2 and CO_2 sorption isotherms of Co-TTPP nanosheets prepared by liquid-liquid interfacial method and (b) pore size distribution profile based on CO_2 adsorption.

Table S1. DNA sequences used in this work.

Oligonucleotide	Sequence
P1	AGACTCTTGAGTTCTCAGTATG-Texas Red
T1 (H5N1)	TCTGAGAACTCAAGAGTCATAC
SM1	TCTGAGAACTCAAGAGTTATAC
DM1	TCTGACAACTCAAGAGTTATAC
R	TAGCTTATCAGACAGATGTTGA
P2	TTCTTCATCGAGAGTGTAGTCG-TET
T2 (H1N1)	AAGAAGTAGCTCTCACATCAGC

Table S2. Comparison of different nanomaterial-based fluorescent DNA sensors.

Type	Detection condition	Limit of detection	Detection time	Multiplexed detection	Reference
Gold nanoparticle	NR[a)]	~nM	minutes	Yes	S8
Sing-wall carbon nanotube	RT[b)]	4 nM	hours	NR	S9
Graphene oxide	RT	≈10 nM	0.5 h	NR	S10
Graphene oxide	NT	100 pM	≈1 min	Yes	S11
Carbon nitride nanosheet	RT	2.1 nM	minutes	Yes	S12
Graphene oxide	RT	800 pM	40 min	NR	S13
MoS_2 single layer	RT	500 pM	minutes	Yes	S14
WS_2 nanosheet	RT	60 pM	0.5 h	Yes	S15
CoP nanowire	RT	100 pM	minutes	NR	S16
Graphdiyne oxide nanosheet	95°C	84 pM	minutes	NR	S17
Free-standing Cu-TCPP nanosheets	RT	20 pM	minutes	Yes	S18
Substrate-supported Co-TTPP nanosheet	RT	120 pM	minutes	Yes	This work

[a)] Not reported; [b)] room temperature

References

S1 C. C. Mark, N. Bampos, S. L. Darling, M. Montalti, L. Prodi and J. K. M. Sanders, *J. Org. Chem.*, 2001, **66**, 4476.

S2 W. Zhao, Y. Huang, Y. Liu, L. Cao, F. Zhang, Y. Guo and B. Zhang, *Chem.-Eur. J.*, 2016, **22**, 15049.

S3 G. Liu, A. N. Khlobystov, G. Charalambidis, A. G. Coutsolelos and G. A. D. Briggs, K. Porfyrakis, *J. Am. Chem. Soc.*, 2012, **134**, 1938.

S4 R. Sakamoto, K. Hoshiko, Q. Liu, T. Yagi, T. Nagayama, S. Kusaka, M. Tsuchiya, Y. Kitagawa, W.-Y. Wong and H. Nishihara, *Nat. Commun.*, 2015, **6**, 6713.

S5 J. P. Perdew, K. Burke and M. Ernzerhof, *Phys. Rev. Lett.*, 1996, **77**, 3865.

S6 G. Kresse and J. Hafner, *J. Phys. Rev. B*, 1993, **48**, 13115.

S7 G. Kresse and J. Furthmüller, J. *Phys. Rev. B*, 1996, **54**, 11169.

S8 B. Dubertret, M. Calame and A. J. Libchaber, *Nat. Biotechnol.*, 2001, **19**, 365.

S9 R. Yang, J. Jin, Y. Chen, N. Shao, H. Kang, Z. Xiao, Z. Tang, Y. Wu, Z. Zhu and W. Tan, *J. Am. Chem. Soc.*, 2008, **130**, 8351.

S10 C.-H. Lu, H.-H. Yang, C.-L. Zhu, X. Chen and G.-N. Chen, *Angew. Chem. Int. Ed.*, 2009, **48**, 4785.

S11 S. He, B. Song, D. Li, C. Zhu, W. Qi, Y. Wen, L. Wang, S. Song, H. Fang and C. Fan, *Adv. Funct. Mater.*, 2010, **20**, 453.

S12 Q. Wang, W. Wang, J. Lei, N. Xu, F. Gao and H. Ju, *Anal. Chem.*, 2013, **85**, 12182.

S13 S. Guo, D. Du, L. Tang, Y. Ning, Q. Yao and G. Zhang, *Analyst*, 2013, **138**, 3216.

S14 C. Zhu, Z. Zeng, H. Li, F. Li, C. Fan and H. Zhang, *J. Am. Chem. Soc.*, 2013, **135**, 5998**.**

S15 Y. Yuan, R. Li and Z. Liu, *Anal. Chem.*, 2014, **86**, 3610.

S16 J. Tian, N. Cheng, Q. Liu, W. Xing and X. Sun, *Angew. Chem. Int. Ed.*, 2015, **54**, 5493.

S17 C. Wang, P. Yu, S. Guo, L. Mao, H. Liu and Y. Li, *Chem. Commun.*, 2016, **52**, 5629.

S18 M. Zhao, Y. Wang, Q. Ma, Y. Huang, X. Zhang, J. Ping, Z. Zhang, Q. Lu, Y. Yu, H. Xu, Y. Zhao and H. Zhang, *Adv. Mater.*, 2015, **27**, 7372.